Marker-less Reconstruction of Dense 4-D Surface Motion Fields Using Active Laser Triangulation for Respiratory Motion Management

S. Bauer[1], B. Berkels[4], S. Ettl[2], O. Arold[2], J. Hornegger[1,3], M. Rumpf[5]

[1]*Pattern Recognition Lab, Dept. of Computer Science*
[2]*Institute of Optics, Information and Photonics*
[3]*Erlangen Graduate School in Advanced Optical Technologies (SAOT)*
***Friedrich-Alexander-Universität Erlangen-Nürnberg**, Erlangen, Germany*
[4]*Interdisciplinary Mathematics Institute, **University of South Carolina**, Columbia, SC, USA*
[5]*Institute for Numerical Simulation, Rheinische **Friedrich-Wilhelms-Universität Bonn**, Bonn, Germany*

MICCAI NICE 2012

MEDICAL VALLEY Europäische Metropolregion Nürnberg

FRIEDRICH-ALEXANDER UNIVERSITÄT ERLANGEN-NÜRNBERG

UNIVERSITY OF SOUTH CAROLINA

universitätbonn

External-Internal Tumor Motion Correlation

- **Hybrid tumor-tracking in image-guided radiation therapy (IGRT):**
  - Continuous monitoring of external respiration surrogate
  - Predict internal tumor position from surrogate using correlation model
  - Low-dim. surrogates cannot depict complexity of respiratory motion
  - Involve patient preparation and reproducible marker placement
- **Goal:** Dense marker-less 4-D motion fields to improve correlation[1,2]

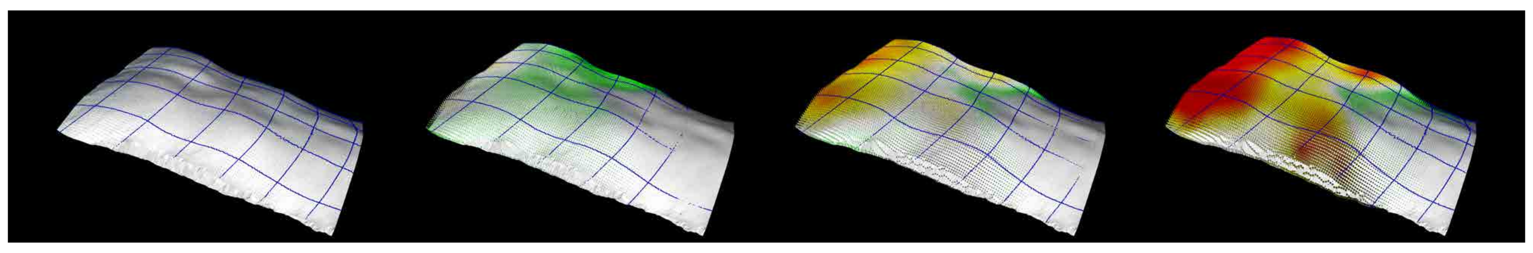

Light Sectioning 2.0

- **Marker-less range imaging (RI) in clinical solutions:**
  - Consecutive laser sweep / light sectioning (C-RAD, LAP)
  - Active stereo vision (VisionRT)
- **Limitations regarding motion management:**
  - Measurement uncertainties (sampling principle)
  - Lack of real-time capability (designed for patient setup)
- **Multi-line active triangulation (AT) sensor[3]:**
  - Accurate 3-D sampling (light sectioning) at 30 Hz
  - Simultaneous sampling of multiple lines in a grid structure
  - Compact housing, inexpensive hardware

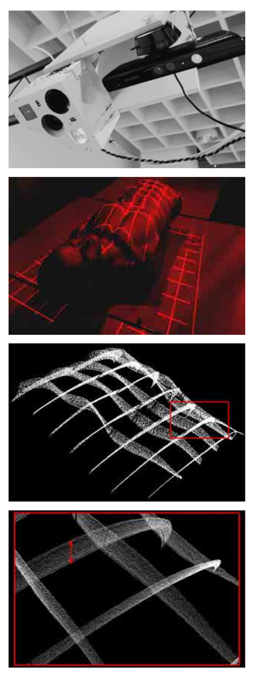

Reconstruction of Dense 4-D Surface Motion Fields from Sparse Data

- **Input:** - Sparse sampling of respiring patient: $Y = \{y_1, \dots, y_n\}, y_i \in \mathbb{R}^3$
  - Dense planning data prior shape: $\mathcal{G} = \{(\zeta, g(\zeta)) \in \mathbb{R}^3 : \zeta \in \Omega\}$

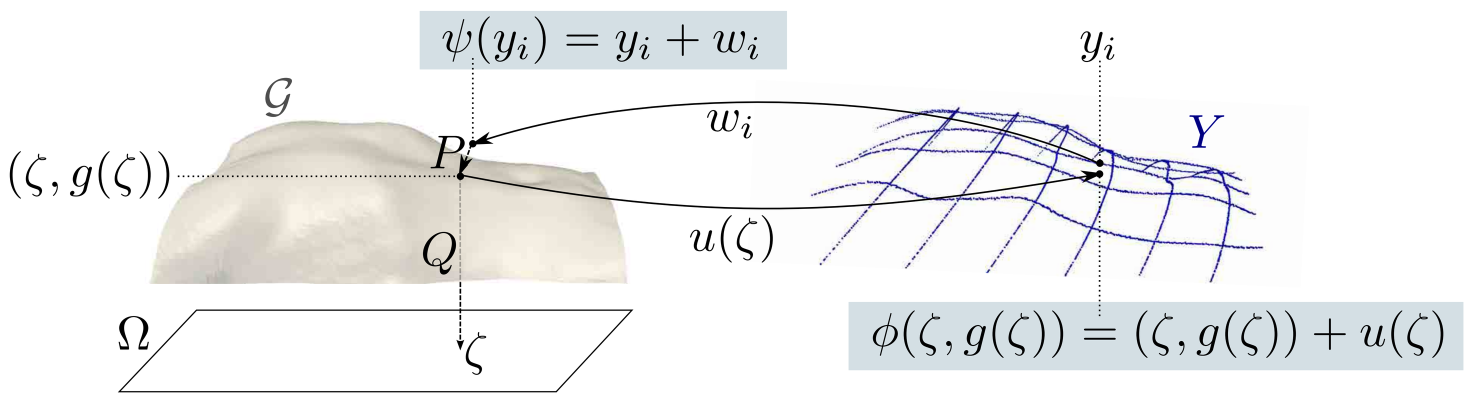

- **Output:** - Dense deformation ϕ of $\mathcal{G}$ with $Y \subset \phi(\mathcal{G}),\ u : \Omega \to \mathbb{R}^3$
  - Sparse deformation ψ of Y with $\psi(Y) \subset \mathcal{G},\ W = \{w_i\},\ w_i \in \mathbb{R}^3$

- **Variational formulation:** $\mathcal{E}_{\mathrm{con}}$ ensures inverse-consistency of ϕ and ψ

$$\mathcal{E}_{\mathrm{match}}[W] := \frac{1}{2n} \sum_{i=1}^{n} |d(y_i + w_i)|^2 \qquad \mathcal{E}_{\mathrm{reg}}[u] := \frac{1}{2} \int_\Omega |\triangle u|^2 \,\mathrm{d}x$$

$$\mathcal{E}[u, W] := \mathcal{E}_{\mathrm{match}}[W] + \kappa\, \mathcal{E}_{\mathrm{con}}[u, W] + \lambda\, \mathcal{E}_{\mathrm{reg}}[u]$$

$$\mathcal{E}_{\mathrm{con}}[u, W] := \frac{1}{2n} \sum_{i=1}^{n} |P(y_i + w_i) + u(Q\, P(y_i + w_i)) - y_i|^2$$

Signed distance function $d(x) := \pm \mathrm{dist}(x, \mathcal{G})$
Projection of a point $x \in \mathbb{R}^3$ onto $\mathcal{G}$: $P(x) := x - d(x)\nabla d(x)$
Orthogonal projection $Q \in \mathbb{R}^{2\times3}$: $Q(\zeta, g(\zeta)) = \zeta$

Experiments and Results

- **Numerical optimization:**
  - Finite Element (FE) discretization
  - Regularized gradient descent scheme
  - Initialization of u with previous estimate
  - Initialization of W with $w_j = P(y_j) - y_j$
- **Experimental setup:**
  - AT prototype[3] with 11x10 line grid (30 Hz)
  - Measurement uncertainty: 0.39 mm
  - Ground truth: structured light (SL) data $\mathcal{M}_p$
- **Dataset:**
  - 16 subjects, abdominal/thoracic, 8 phases
- **Evaluation metric:** $|\mathrm{dist}(\phi_p(\mathcal{G}), \mathcal{M}_p)|$

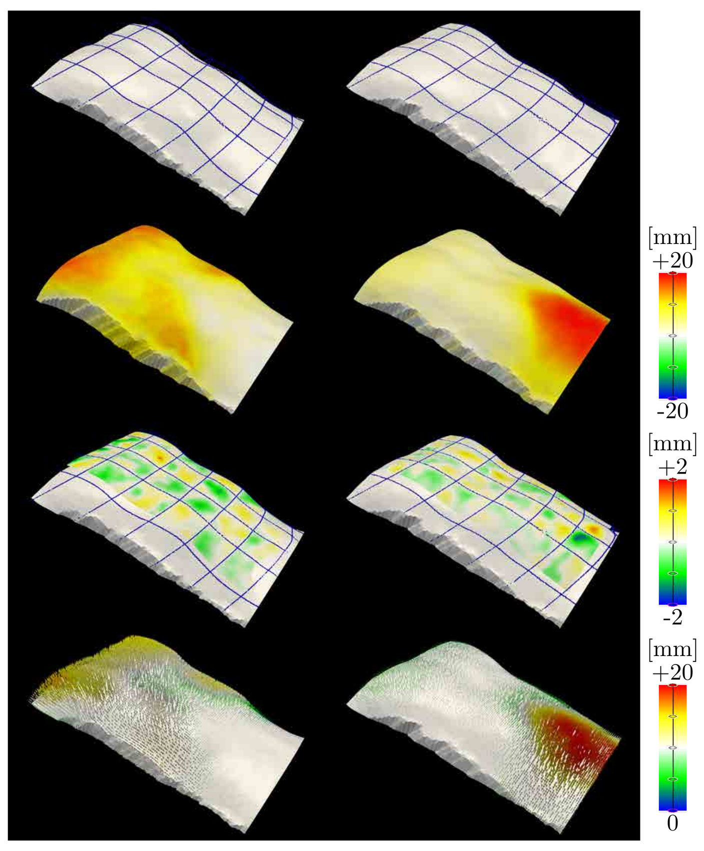

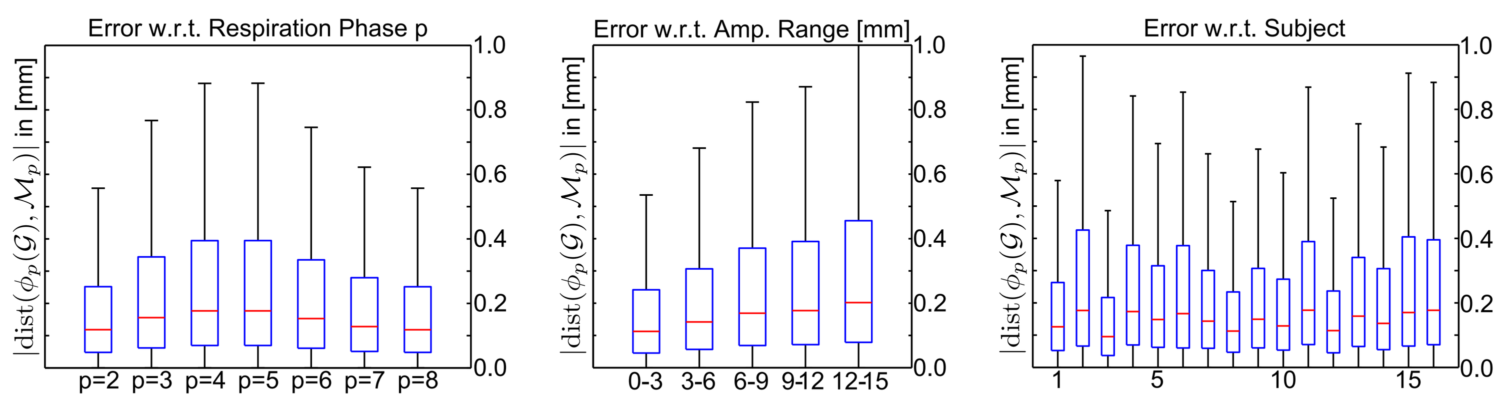

Fig. 1: Boxplots of residual surface mismatch $|\mathrm{dist}(\phi_p(\mathcal{G}), \mathcal{M}_p)|$ for realistic AT sampling data from 16 subjects, for thoracic respiration, one cycle is divided into eight phases.

- **Quantitative evaluation on realistic AT data:**
  - Synthetic sampling of dense SL surface data using an AT simulator
  - Incorporation of sensor-specific noise characteristics → realistic data
  - Mean reconstruction error: ±0.22 mm
  - Runtime performance: < 3 s (motion field density: 16k, 2.7 GHz CPU)

Conclusions

- Novel variational framework for sparse-to-dense surface registration
- Reliable reconstruction of 4-D motion fields, even with strong respiration
- Applications in IGRT: external-internal tumor motion correlation modeling, motion-compensated patient positioning[4]
- Potential for motion-compensated tomographic reconstruction and image-guided interventions

Acknowledgments: The authors gratefully acknowledge the support by the European Regional Development Fund (ERDF) and the Bayerisches Staatsministerium für Wirtschaft, Infrastruktur, Verkehr und Technologie (StMWIVT) under Grant No. IUK338/001.

References

[1] J. Schaerer, A. Fassi, M. Riboldi, P. Cerveri, G. Baroni, D. Sarrut. *Multi-dimensional respiratory motion tracking from markerless optical surface imaging based on deformable mesh registration.* Phys Med Biol 57(2) (2012) pp. 357-373

[2] S. Bauer, B. Berkels, J. Hornegger, M. Rumpf. *Joint ToF image denoising and registration with a CT surface in radiation therapy.* Proceeding of SSVM, LNCS 6667, Springer (2012) pp. 98-109

[3] S. Ettl, O. Arold, Z. Yang, G. Häusler. *Flying triangulation - an optical 3D sensor for the motion-robust acquisition of complex objects.* Appl Opt 51(2), 2012, 218-289

[4] J. Wasza, S. Bauer, J. Hornegger. *Real-time motion compensated patient positioning and non-rigid deformation estimation using 4-D shape priors.* Proceedings of MICCAI, LNCS 7511, Springer (2012) pp. 576-583